

LETTER • OPEN ACCESS

## Disproportionate exposure to surface-urban heat islands across vulnerable populations in Lima city, Peru

To cite this article: Edson J Ascencio *et al* 2023 *Environ. Res. Lett.* **18** 074001

View the [article online](#) for updates and enhancements.

You may also like

- [Reduction in human activity can enhance the urban heat island: insights from the COVID-19 lockdown](#)

TC Chakraborty, Chandan Sarangi and Xuhui Lee

- [Monitoring Urban Heat Island Spatial Variability over Urban Structure Types – A Case Study from a Fast-growing City in the Vietnamese Mekong Delta](#)

N. K. Diem, P. K. Diem, P. M. Thien et al.

- [Decline in surface urban heat island intensity in India during heatwaves](#)

Rahul Kumar and Vimal Mishra

The advertisement features a blue background with circular ECS logos at the top and bottom. In the center, there's a photo of a smiling woman in a tan blazer. To her left, text details the meeting: "248th ECS Meeting Chicago, IL October 12-16, 2025 Hilton Chicago". To her right, large text reads "Science + Technology + YOU!". At the bottom, a button says "REGISTER NOW". On the far right, text encourages early registration: "Register by September 22 to save \$\$".

**UNITED THROUGH SCIENCE & TECHNOLOGY**

**ECS** The Electrochemical Society  
Advancing solid state & electrochemical science & technology

**248th ECS Meeting**  
Chicago, IL  
October 12-16, 2025  
Hilton Chicago

**Science + Technology + YOU!**

**REGISTER NOW**

Register by September 22 to save \$\$

# ENVIRONMENTAL RESEARCH LETTERS



OPEN ACCESS

RECEIVED  
6 January 2023REVISED  
23 May 2023ACCEPTED FOR PUBLICATION  
8 June 2023PUBLISHED  
16 June 2023

Original content from this work may be used under the terms of the Creative Commons Attribution 4.0 licence.

Any further distribution of this work must maintain attribution to the author(s) and the title of the work, journal citation and DOI.



## LETTER

# Disproportionate exposure to surface-urban heat islands across vulnerable populations in Lima city, Peru

Edson J Ascencio<sup>1</sup> , Antony Barja<sup>1</sup> , Tarik Benmarhnia<sup>2</sup> and Gabriel Carrasco-Escobar<sup>1,2,\*</sup>

<sup>1</sup> Health Innovation Laboratory, Institute of Tropical Medicine 'Alexander von Humboldt', Universidad Peruana Cayetano Heredia, Lima, Peru

<sup>2</sup> Scripps Institution of Oceanography, University of California San Diego, La Jolla, CA, United States of America

\* Author to whom any correspondence should be addressed.

E-mail: [gabriel.carrasco@upch.pe](mailto:gabriel.carrasco@upch.pe)

**Keywords:** temperature, socioeconomic inequity, urban heat island

Supplementary material for this article is available [online](#)

## Abstract

Climate change constitutes an unprecedented challenge for public health and one of its main direct effects are extreme temperatures. It varies between intra-urban areas and this difference is called surface urban heat island (SUHI) effect. We aimed to assess SUHI distribution among socioeconomic levels in Lima, Peru by conducting a cross-sectional study at the block-level. The mean land surface temperature (LST) from 2017 to 2021 were estimated using the TIRS sensor (Landsat-8 satellite [0.5 km scale]) and extracted to block level. SUHI was calculated based on the difference on mean LST values (2017–2021) per block and the lowest LST registered in a block. Socioeconomic data were obtained from the 2017 Peruvian census. A principal component analysis was performed to construct a socioeconomic index and a mixture analysis based on quantile g-computation was conducted to estimate the joint and specific effects of socioeconomic variables on SUHI. A total of 69 618 blocks were included in the analysis. In the Metropolitan Lima area, the mean SUHI estimation per block was 6.44 (SD = 1.44) Celsius degrees. We found that blocks with high socioeconomic status (SES) showed a decreased exposure to SUHI, compared to those blocks where the low SES were predominant ( $p$ -value < 0.001) and that there is a significant SUHI exposure variation ( $p$ -value < 0.001) between predominant ethnicities per block (Non-White, Afro-American, and White ethnicities). The mixture analysis showed that the overall mixture effect estimates on SUHI was -1.01 (effect on SUHI of increasing simultaneously every socioeconomic variable by one quantile). Our study highlighted that populations with low SES are more likely to be exposed to higher levels of SUHI compared to those who have a higher SES and illustrates the importance to consider SES inequalities when designing urban adaptation strategies aiming at reducing exposure to SUHI.

## 1. Introduction

It is now recognized that climate change constitutes an unprecedented challenge for public health and that societal impacts are disproportionately impacting communities with low socio-economic resources [1–3]. The World Health Organization predicts more than five million additional deaths between 2030 and 2050 from climate change worldwide and more than 400 000 additional deaths in Latin America [4], a region where socioeconomic and health care access

inequalities exacerbates such impacts [5]. People in poverty and minority groups have exacerbated challenges accessing health care, which prevents them to be diagnosed, treated, and rehabilitated from climate-related health conditions [6]. As one of the main direct effects of climate change, extreme temperatures impact human health by compromising the body's ability to regulate its internal temperature, worsening diabetes-related conditions, and cerebrovascular, respiratory, and cardiovascular diseases [7]. In 2019, the number of heat-related attributable deaths worldwide

in urban and non-urban settings increased by 151 000 compared to 1990, and it is expected to grow as temperatures increases [8].

In Latin America, one of the most inequitable regions in the world [9, 10], a five- to ten-fold increase in the frequency of extremely hot days (95th percentile of daily mean temperature between 1961 and 1990) and in the number of heat waves per season in the largest cities of South America (i.e. Bogota, Caracas, Fortaleza, Guayaquil, Iquique, Lima, Mérida, Rochambeau, San Fernando, São Paulo) is projected by the mid of this century [11]. Peru, located in Latin America, is one of the most affected countries by the temperature increase [12]; in addition, it is a country with one of the highest proportions (more than 70%) of heat-related mortality attributed to human-induced climate change [13]. In this country, annually, there is a range of 442–3644 deaths in each Peruvian city due to extreme temperatures [14].

Yet, this rise of temperature and surface temperature is especially marked in urban areas compared with the surrounding suburban and rural areas or even in the same within urban areas [15–17]. The difference between the urban and rural areas' energy balance is called the surface urban heat island (SUHI) effect [18, 19]. Evidence shows that the global increase in heat intensity and mean temperatures affects the urban inhabitants' physical and mental health, increasing the heat-related morbidity (dehydration, heat strokes, loss of labor productivity, and decreased learning) [20–25] and mortality (suicide rates, myocardial infarction, hyperthermia, and shock) [26–30]. Therefore, SUHI affects focalized urban populations due to its high temperature exposure. This phenomenon is particularly important in Latin America, a region where more than 80% of the total population lives in urban areas and [31], by 2050, will be the most urbanized region in the world (91.4% population living in urban areas) [32]. In addition, a previous review of racial and socioeconomic disparities and heat-related health effects describes that ethnic minority groups or populations of low socioeconomic status (SES) may be more vulnerable to the effect of heat and that more studies are needed to accurately identify the most exposed target populations [33].

In Latin America, some studies that explored the relationship between temperature and urbanization were carried out in the largest cities [34–58] showing a SUHI ranging between 0.5 °C and 15 °C. In Lima, previous descriptive studies estimated urban heat island (UHI) effect and SUHI first at city-level [59–61] and then downscaling to district-level [62], showing that urban areas are more exposed than rural areas. Despite its key relevance in developing countries, most studies showing how UHI and SUHI effect are not equally distributed in urban areas were carried out in high-income countries [63].

An adequate SUHI documentation is highly relevant for environmental justice implications and designing equitable adaptation strategies, especially nowadays where climate change context increases SUHI impact [64]. To date, no studies that describes how SUHI are unequally distributed across the socioeconomic gradient were conducted in Latin America [33, 65].

This study aims to assess the SUHI distribution among socioeconomic levels at a fine-scale level in Lima, a city with the highest concentration of population and socioeconomic inequality in Peru [66]. We focus on a large set of SES variables and propose two distinct approaches based on: (1) a composite SES index and (2) a quantile g-computation model. In this paper, we rely of land surface temperature (LST) estimates to approximate local variations in temperatures across neighborhoods and characterize spatial variability of SUHI in this region as typically done in recent papers in other geographical contexts [67–70]. However, such remote sensing product is only a proxy of local variations in air temperatures which was not available for this study setting. Our study is innovative by being the first approach to SUHI and SES relationship at a granular level in Peru, the fourth most unequal country in the world [71]. Evidence provided by our study could improve the early detection of socioeconomically disadvantaged populations, especially the ones that could be exposed to higher temperatures and in consequence, harmful health effects to improve an equitable adaptation strategy.

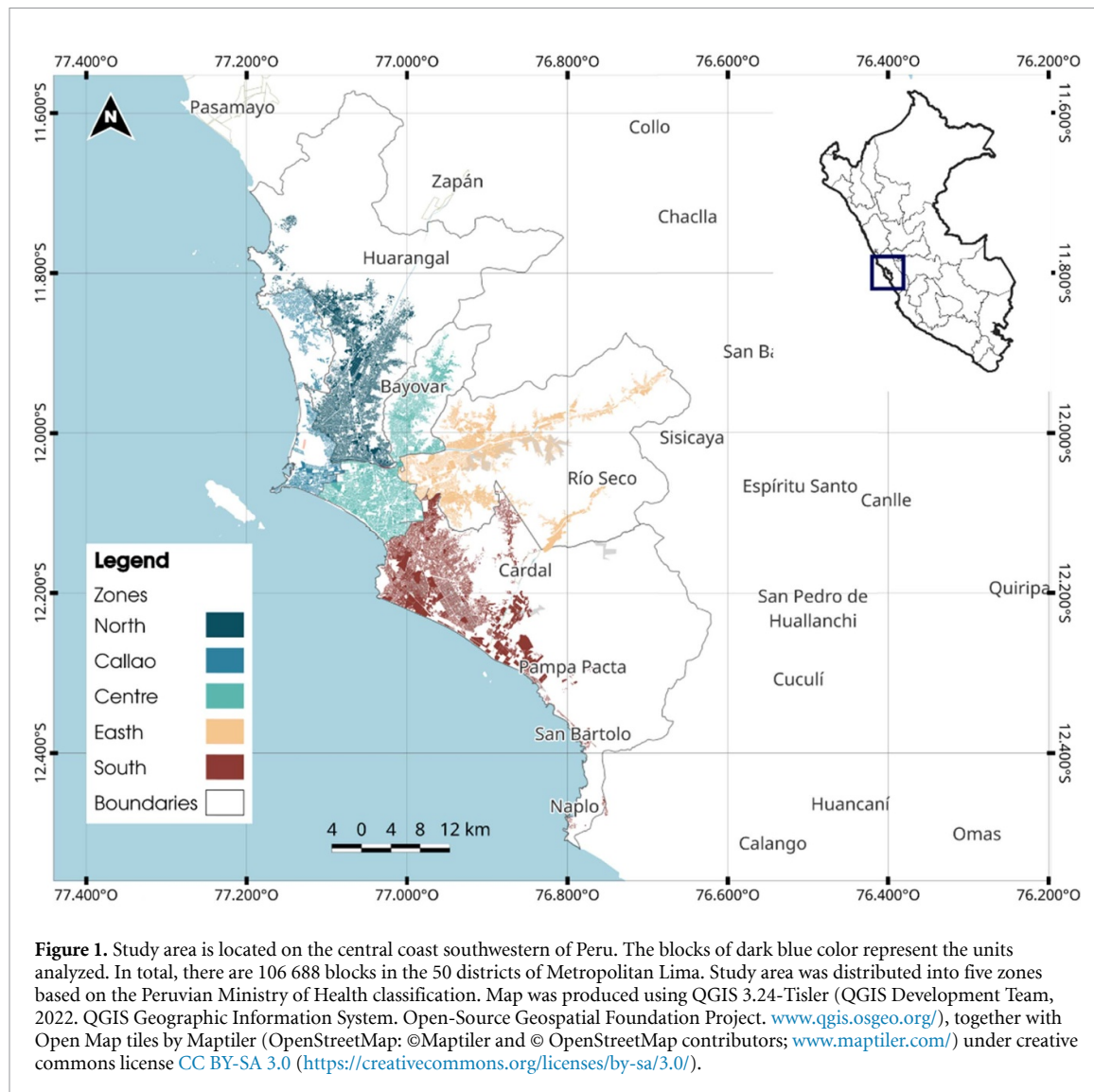
## 2. Method

### 2.1. Study design

A cross-sectional ecological study was conducted in Lima, Peru using fine-scale data to conduct a block-level analysis (9569 470 population) [72]. Baseline socioeconomic data were obtained from the most recent Peruvian census (2017), carried out by the Peruvian National Institute of Statistics and Informatics (INEI by its Spanish acronym). SUHI was estimated using the 2017–2021 mean daytime temperature based on satellite products. We constructed a SES index and conducted a quantile g-computation analysis to estimate the joint and individual effects of SES variables on SUHI.

### 2.2. Study area and population

Metropolitan Lima (comprising the Lima province and the Callao constitutional province) has an area of 2840.35 km<sup>2</sup> with a total population of 9569 470 [72] and an average altitude of 557.72 m above sea level. Metropolitan Lima is characterized by a warm arid climate [73] throughout the year with maximum temperatures of 19 and 31 Celsius degrees in the Southern and Northern regions, respectively (according to the Warren Thorntwaite classification) [74]. We divided the districts in the Metropolitan Lima area into five zones based on the territory divisions of the



Peruvian Ministry of Health [75] (figure 1): Callao (7 districts: Bellavista, Callao, Carmen de la Legua Reynoso, La Perla, La Punta, Mi Perú, and Ventanilla), Center (14 districts: San Juan de Lurigancho, San Borja, La Victoria, San Luis, Surquillo, Lince, San Isidro, Miraflores, Magdalena del Mar, San Miguel, Jesús María, Breña, Lima, and Pueblo Libre), East (7 districts: Ate, Chaclacayo, Cieneguilla, El Agustino, La Molina, Lurigancho, and Santa Anita), North (9 districts: Ancon, Santa Rosa, Puente Piedra, Los Olivos, San Martín de Porres, Rimac, Independencia, Comas, and Carabayllo), and South (13 districts: Villa María del Triunfo, San Juan de Miraflores, Villa el Salvador, Lurín, Pucusana, Punta Hermosa, Punta Negra, San Bartolo, Santa María del Mar, Pachacamac, Chorrillos, Barranco, and Santiago de Surco) (tables 1 and S1).

### 2.3. Data sources

In Metropolitan Lima, 106 688 blocks were registered; however, of these, 35 400 blocks (33.18% of total) had no available socioeconomic data due to a lack of

inhabited blocks or blocks with fewer than 30 inhabitants, whose data was restricted by the source census 2017 to maintain resident privacy. A total of 69 618 blocks were included in the analysis and details of the blocks' selection are shown in figure S1.

#### 2.3.1. Socioeconomic variables

Census data was provided by INEI via the REDATAM platform [72]. Information from the 2017 Census was used to collect socioeconomic variables. In the census, all inhabitants were asked to report the district where they are currently living (2016–2017), which type of housing they are currently living in, access to water, electric energy, and internet services, and whether they had health insurance or not, grade of literacy and highest education, ethnicity that participant's identified with, whether they are able to work or not, and if they have recently received income (from any source). Socioeconomic variables were processed as the percentage of population who have certain socioeconomic characteristic per block. For example, the health insurance access variable represents the

**Table 1.** General characteristics of the study population.

Characteristics per block	Metropolitan Lima (total) (N = 69 618)	Zones in Metropolitan Lima			
		Callao zone (N = 8011)	Center zone (N = 14 702)	East zone (N = 11 467)	North zone (N = 19 259)
Population per block	130 (147) 97.0 [53.0, 167]	120 (129) 89.0 [55.0, 151]	156 (213) 116 [59.0, 199]	118 (118) 81.0 [48.0, 149]	129 (132) 96.0 [52.0, 172] 101 [55.0, 155]
Per capita income per block	936 (460) 813 [642, 1010]	789 (295) 713 [531, 975]	1210 (700) 925 [666, 1680]	911 (391) 808 [629, 1000]	775 (203) 750 [617, 916] 966 (392) 840 [732, 1010]
Surface urban heat island (SUHI) per block (°C)	6.31 (1.14) 6.19 [5.71, 6.99]	6.27 (1.76) 6.41 [5.19, 7.43]	7.17 (1.11) 6.96 [6.39, 7.74]	6.02 (1.29) 5.87 [5.15, 6.86]	6.63 (1.39) 6.62 [5.69, 7.47]
SUHI during summer per block (°C)	9.11 (0.948) 9.09 [8.56, 9.68]	9.08 (1.53) 9.19 [8.26, 10.1]	9.77 (0.929) 9.64 [9.16, 10.2]	8.94 (1.18) 8.87 [8.06, 9.75]	9.56 (1.20) 9.50 [8.76, 10.3]
SUHI during winter per block (°C)	5.15 (2.08) 4.80 [3.61, 6.10]	4.90 (1.91) 4.97 [3.70, 6.26]	4.93 (1.98) 4.76 [3.80, 5.83]	4.79 (1.79) 5.19 [3.93, 6.55]	5.18 (2.20) 5.79 [4.42, 7.22] 5.13 [3.91, 6.48]
Land surface temperature mean (2017)	25.3 (1.34) 25.2 [24.6, 26.0]	24.6 (2.97) 25.3 [22.6, 26.8]	26.5 (1.35) 26.3 [25.6, 27.2]	25.6 (1.57) 25.7 [25.0, 26.4]	24.1 (2.92) 24.1 [22.1, 26.3]
Land surface temperature mean (2021)	26.8 (1.64) 26.6 [25.7, 28.0]	27.3 (1.77) 27.4 [25.9, 28.7]	27.9 (1.30) 27.8 [27.0, 28.7]	27.0 (1.14) 27.0 [26.2, 27.8]	27.1 (1.45) 27.0 [26.2, 28.0]
Land surface temperature mean variation (2021–2017)	1.48 (1.68) 1.16 [0.296, 2.58]	2.75 (2.18) 2.05 [1.16, 3.97]	1.35 (1.06) 1.28 [0.63], 1.95	1.41 (1.90) 1.28 [0.21, 2.18]	3.03 (2.44) 2.70 [0.972, 5.00]
% of female gender per block	51.3 (4.90) 51.4 [48.4, 54.2]	51.1 (4.83) 51.3 [48.3, 54.1]	51.9 (4.93) 52.0 [49.0, 54.9]	51.1 (5.12) 51.2 [48.1, 54.2]	51.0 (4.69) 51.1 [48.3, 53.8] 51.2 [48.2, 54.2]
% of male gender per block	48.7 (4.90) 48.6 [45.8, 51.6]	48.9 (4.83) 48.8 [45.9, 51.7]	48.1 (4.93) 48.0 [45.1, 51.0]	48.9 (5.12) 48.8 [45.8, 51.9]	49.0 (4.69) 48.9 [46.3, 51.7] 48.8 (4.95) 48.7 [45.8, 51.8]

(Continued.)

Table 1. (Continued.)

Characteristics per block	Metropolitan Lima (total) (N = 69 618)	Zones in Metropolitan Lima			
		Callao zone (N = 8011)	Center zone (N = 14 702)	East zone (N = 11 467)	North zone (N = 19 259)
<b>% of population aged 0–14 per block</b>					
Mean (SD)	24.0 (8.01) 23.5 [18.5, 28.9]	26.6 (7.99) 26.0 [20.8, 32.0]	21.3 (8.50) 20.2 [15.3, 26.4]	24.8 (7.83) 24.4 [19.5, 29.6]	24.9 (7.34) 24.1 [19.9, 29.2]
Median [Q1, Q3]					23.5 (7.72) 23.2 [18.3, 28.1]
<b>% of population aged 15–29 per block</b>					
Mean (SD)	25.9 (6.75) 25.4 [21.4, 29.9]	25.2 (6.34) 24.7 [21.0, 28.9]	25.0 (7.04) 24.4 [20.3, 29.1]	26.7 (6.85) 26.5 [22.2, 30.9]	26.2 (6.44) 25.7 [22.0, 30.0]
Median [Q1, Q3]					25.9 (6.86) 25.4 [21.3, 30.0]
<b>% of population aged 30–64 per block</b>					
Mean (SD)	42.3 (6.33) 42.7 [38.6, 46.3]	41.0 (6.17) 41.5 [37.2, 45.1]	43.5 (6.56) 44.0 [39.9, 47.7]	41.6 (6.39) 41.8 [37.6, 45.8]	41.9 (5.94) 42.4 [38.5, 45.6]
Median [Q1, Q3]					42.9 (6.33) 43.2 [39.2, 46.9]
<b>% of population aged 65 or over per block</b>					
Mean (SD)	7.83 (6.18) 6.58 [3.03, 11.4]	7.18 (5.89) 5.79 [2.63, 10.6]	10.2 (7.56) 9.22 [3.92, 15.3]	6.87 (5.59) 5.76 [12.82, 9.68]	7.01 (4.96) 6.32 [3.13, 10.3]
Median [Q1, Q3]					7.68 (6.09) 6.45 [2.86, 11.4]
<b>Socioeconomic characteristics</b>					
<b>% of permanent address at house or apartment per block</b>					
Mean (SD)	97.4 (8.67) 100 [100, 100]	98.0 (7.64) 100 [100, 100]	95.2 (12.1) 100 [98.0, 100]	97.6 (8.03) 100 [100, 100]	98.2 (6.76) 100 [100, 100]
Median [Q1, Q3]					97.9 (7.44) 100 [100, 100]
<b>% of access to public water service per block</b>					
Mean (SD)	72.7 (29.6) 87.5 [80.8, 87.5]	72.0 (28.1) 87.5 [72.3, 87.5]	76.1 (26.6) 87.5 [85.7, 87.5]	68.7 (33.2) 87.5 [71.6, 87.5]	73.4 (28.7) 87.5 [81.1, 87.5]
Median [Q1, Q3]					72.0 (30.9) 87.5 [81.4, 87.5]
<b>% of access to electric energy service per block</b>					
Mean (SD)	83.3 (13.1) 87.5 [87.2, 87.5]	85.4 (8.32) 87.5 [87.5, 87.5]	84.2 (11.0) 87.5 [87.2, 87.5]	80.9 (17.0) 87.5 [86.2, 87.5]	83.5 (12.3) 87.5 [87.2, 87.5]
Median [Q1, Q3]					82.9 (14.4) 87.5 [87.5, 87.5]
<b>% of access to internet service per block</b>					
Mean (SD)	43.3 (26.0) 42.4 [23.2, 61.8]	38.8 (23.9) 37.5 [18.9, 57.0]	51.6 (29.0) 52.0 [28.3, 78.5]	40.4 (26.4) 37.9 [20.2, 56.9]	40.2 (22.7) 41.4 [22.7, 57.7]
Median [Q1, Q3]					43.7 (25.6) 42.6 [25.1, 60.5]
<b>% of access to health insurance per block</b>					
Mean (SD)	69.5 (10.3) 70.0 [63.3, 76.5]	74.3 (8.41) 75.0 [69.7, 79.9]	71.5 (10.2) 71.8 [65.0, 78.8]	65.9 (11.6) 66.0 [58.6, 73.7]	68.0 (9.56) 68.7 [62.6, 74.1]
Median [Q1, Q3]					69.8 (9.91) 70.0 [63.9, 76.2]

(Continued.)

Table 1. (Continued.)

	Metropolitan Lima (total) (N = 69 618)	Zones in Metropolitan Lima			
		Callao zone (N = 8011)	Center zone (N = 14 702)	East zone (N = 11 467)	North zone (N = 19 259)
Characteristics per block					
% of literacy population per block	85.7 (5.18) Mean (SD) Median [Q1, Q3]	84.7 (5.18) 85.1 [81.6, 88.3]	87.0 (5.28) 87.9 [84.1, 90.8]	85.0 (5.38) 85.5 [81.8, 88.6]	85.2 (4.97) 85.9 [82.5, 88.6]
% of people with higher education level per block	29.6 (18.0) Mean (SD) Median [Q1, Q3]	25.0 (14.9) 22.1 [13.6, 34.0]	36.7 (22.1) 33.0 [17.8, 57.9]	28.0 (18.0) 24.4 [14.5, 36.8]	27.1 (13.8) 26.7 [16.4, 36.8]
% of people without education per block	2.93 (2.60) Mean (SD) Median [Q1, Q3]	3.04 (2.74) 2.49 [1.25, 4.17]	2.55 (2.48) 2.00 [0.913, 3.51]	3.27 (2.76) 2.70 [1.41, 4.62]	3.07 (2.63) 2.52 [1.37, 4.17]
% of people with basic school education level per block	67.5 (17.1) Mean (SD) Median [Q1, Q3]	72.0 (14.1) 74.6 [63.6, 82.5]	60.8 (21.1) 64.3 [40.7, 78.5]	68.7 (17.0) 72.0 [60.5, 81.3]	69.8 (13.1) 70.2 [60.7, 79.6]
% of people who are at least 15 years old and able to work per block	66.5 (6.97) Mean (SD) Median [Q1, Q3]	64.3 (6.96) 64.7 [59.6, 69.3]	68.8 (7.40) 69.8 [64.4, 74.1]	65.8 (6.81) 66.2 [61.7, 70.5]	65.7 (6.39) 66.4 [62.0, 70.1]
% of people who recently received income per block	43.1 (8.57) Mean (SD) Median [Q1, Q3]	39.8 (8.16) 40.5 [35.3, 45.1]	45.5 (8.38) 46.3 [41.1, 50.8]	42.9 (8.95) 44.0 [38.2, 48.7]	41.6 (8.17) 42.4 [37.3, 46.8]
% of White ethnicity per block	5.58 (5.94) Mean (SD) Median [Q1, Q3]	5.81 (4.90) 4.97 [2.42, 8.11]	7.27 (7.92) 5.33 [2.52, 9.01]	4.53 (5.37) 3.14 [1.12, 6.06]	4.95 (4.31) 4.17 [2.01, 6.87]
% of Mestizo ethnicity per block	53.5 (14.9) Mean (SD) Median [Q1, Q3]	55.1 (13.2) 56.8 [47.4, 64.4]	54.7 (14.9) 57.1 [46.3, 65.4]	48.8 (16.5) 50.4 [38.6, 60.9]	55.0 (13.8) 57.1 [47.4, 64.5]
% of Afro-American ethnicity per block	2.25 (2.99) Mean (SD) Median [Q1, Q3]	3.53 (3.85) 2.58 [0.725, 5.10]	2.07 (2.64) 1.39 [0, 2.88]	1.69 (2.60) 0.909 [0, 2.44]	2.30 (2.96) 1.54 [0, 3.22]
% of Native ethnicity per block	15.2 (12.4) Mean (SD) Median [Q1, Q3]	10.1 (9.32) 7.77 [3.23, 14.3]	14.2 (12.2) 11.0 [4.94, 20.5]	21.1 (14.5) 18.7 [10.0, 29.4]	13.9 (10.4) 11.6 [6.51, 18.6]

N, number of blocks; SD, standard deviation; Q1, quartile 1; Q3, quartile 3.

proportion of how many people in each block have any health insurance. In addition, the income per capita was estimated by the INEI 2007 baseline information. Finally, the 2017 blocks' spatial geometries were provided by INEI.

REDATAM exported data were formatted and processed using R software v.4.2.1 (R Core Team (2019). R: A language and environment for statistical computing. R Foundation for Statistical Computing, Vienna, Austria. URL [www.R-project.org](http://www.R-project.org)).

### 2.3.2. Temperature and SUHI estimation

The mean LST data from 2017 to 2021 were estimated using the TIRS sensor of the Landsat 8 satellite at a spatial resolution of  $30\text{ m}^2$  per pixel. These data were provided by the US Geological Survey and are available in the Google Earth Engine (GEE) data catalogue. GEE is a cloud-based platform that allows users to access high-performance computing resources for processing and analyzing large remote sensing datasets [76]. During the 2017–2021 period, a total of 325 images were obtained in GEE for our study area. Landsat's thermal infrared bands were used to estimate LST based on formulas established by Ermida *et al* [77]. These formulas, used by the National Aeronautics and Space Administration (NASA) [78] to calculate LST, were packed in JavaScript and introduced into GEE by its code editor. To remove the presence of cloudiness, all images were processed with the cloud mask function, and then a single image was composed as a result of the mean of all LST values per pixel along 325 images. All satellite image processing was conducted in the code editor of GEE. Finally, the average LST values were extracted per block using the zonal statistic functions of QGIS [79].

At this stage, we obtained the mean LST values (2017–2021) per block. The calculation of the SUHI for each block within Metropolitan Lima was calculated based on the mean LST value per block minus the lowest LST mean value ( $19.5\text{ }^\circ\text{C}$ ) within all study area. The LST and SUHI data processing is described in figure 2. Finally, SUHI (2017–2021) during summer (from 21 December to 21 March) and winter (from 21 June to 23 September) periods was estimated to better understand SUHI effects.

## 2.4. Statistical analysis

First, the characteristics of the study population were summarized using means and standard deviations (SDs) or median and interquartile range for numeric variables, depending on the skewness of their distribution. To compare differences between socioeconomic groups (characteristics defined as the most frequent socioeconomic condition per block) we used the *t*-test or Mann-Whitney *U* tests (for dichotomous categories); and the ANOVA or Kruskal-Wallis tests (for polythomic categories), depending on the assumptions fulfilled for each variable.

### 2.4.1. Composite socioeconomic index (SI)

A principal component analysis (PCA) was performed to construct a SI by taking into account the principal components that, linearly joint, explained more than 80% of the variance. To conduct the PCA, we considered the proportion of the population which presents each socioeconomic characteristic listed above (i.e. type of housing, access to water, electric energy, internet, and health insurance, grade of literacy and highest education, ethnicity, income per capita, whether participants are able to work or not, and if they have recently received income) per block.

### 2.4.2. Quantile g-computation model

Finally, we conducted a quantile g-computation analysis to estimate the joint and individual effects of socioeconomic variables on SUHI estimation in all the study area and stratified by Metropolitan Lima zones. The quantile g-computation estimates the parameters that characterize the change in SUHI estimations given a joint intervention on all exposures, simultaneously (i.e. by increasing all exposures in the mixture by one quantile) [80]. As compared to other mixtures approaches such as weighted quantile sum regressions, the quantile g-computation method allows relationships to go in both positive and negative directions [80].

## 3. Results

### 3.1. Spatial environmental characteristics and socioeconomic factors

The mean population per block was 130 individuals ( $SD = 147$ ), the mean LST variation between 2021 and 2017 per block was  $2.02$  ( $SD = 2.11$ ) Celsius degrees ( $^\circ\text{C}$ ), and the mean SUHI estimation per block was  $6.44\text{ }^\circ\text{C}$  ( $SD = 1.44$ ). During summer and winter periods, SUHI estimation per block was  $9.11\text{ }^\circ\text{C}$  ( $SD = 0.95$ ) and  $4.90\text{ }^\circ\text{C}$  ( $SD = 1.91$ ), respectively. Center and East zones had the highest (156 [ $SD = 213$ ]) and lowest (118 [ $SD = 118$ ]) mean population per block, respectively. East and North zones had the highest (7.17 [ $SD = 1.11$ ]) and lowest (6.02 [ $SD = 1.29$ ]) SUHI estimations. In terms of socioeconomic characteristics in Metropolitan Lima, the mean per capita income per block was 936 ( $SD = 460$ ) Peruvian soles (PEN) or 242 United States dollars (USD), and the mean percentage of the population with a higher degree of education level, basic degree of education level, and without education per block was 29.6 ( $SD = 18.0$ ), 67.5 ( $SD = 17.1$ ), and 2.93 ( $SD = 2.60$ ), respectively. Center zone had the highest mean per capita income per block (1210 PEN [ $SD = 700$ ] or 313 USD), and the North zone had the lowest mean per capita income per block (775 PEN [ $SD = 203$ ] or 200.5 USD) (table 1).

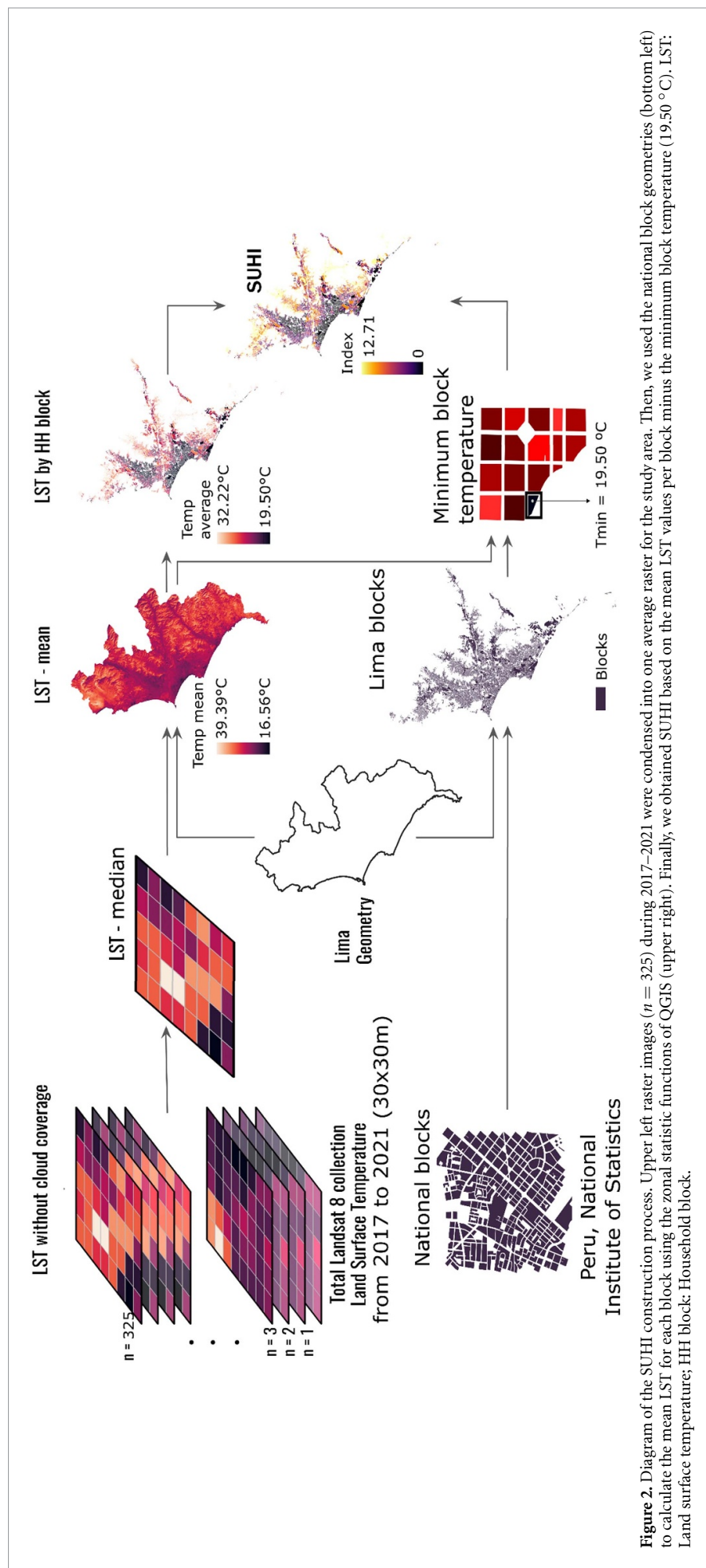


**Figure 2.** Diagram of the SUHI construction process. Upper left raster images ( $n = 325$ ) during 2017–2021 were condensed into one average raster for the study area. Then, we used the national block geometries (bottom left) to calculate the mean LST for each block using the zonal statistic functions of QGIS (upper right). Finally, we obtained SUHI based on the mean LST values per block minus the minimum block temperature ( $19.50^{\circ}\text{C}$ ). LST: Land surface temperature; HH block: Household block.

### 3.2. SUHI distribution per socioeconomic characteristics

SUHI estimate variations were observed when stratified by socioeconomic variables ( $p$ -value < 0.001), which were used in the construction of the SI, as shown in figures 3, 4, S2 and S3. We found that the socioeconomic characteristic representing a favorable SES (i.e. availability of electric energy, water, and internet service, health insurance, access to a permanent home, and higher educational level) showed a lower exposure to SUHI estimation, compared to those blocks characterized by low SES characteristic where predominant ( $p$ -value < 0.001) (figures 3 and S2). In addition, we found that there is a significant SUHI exposure variation ( $p$ -value < 0.001) between predominant ethnicities per block (Non-White Native, Afro-American, Non-White Mestizo, and White ethnicities) (figures 3 and S2). Finally, we evaluated the exposure of SUHI per quantile ranks of socioeconomic characteristics and found that blocks with the lowest quantile ranks of socioeconomic characteristics and high concentration of Native population are significantly ( $p$ -value < 0.001) exposed to high SUHI rates (figures 4 and S3). Those findings on SUHI exposure were consistent during summer (figure S4); however, no clear pattern of SUHI exposure was identified during winter (figure S5).

### 3.3. SI and quantile g-computation on SUHI estimation

We constructed a SI based on a PCA considering 11 socioeconomic variables. Figure S6 shows the contribution of each socioeconomic variable to the two main dimensions of the PCA analysis. We used the index to map the co-distribution of SUHI and Socioeconomic strata (using the SI) as is shown in figure 5. We found that most of the blocks with high SES (based on SI) and low SUHI exposure (13 083 blocks [18.79% of the total]) are localized in the main urban centralized area of Lima. On the other hand, most of the blocks with low SES (based on SI) and high SUHI exposure (12 407 blocks [17.82% of the total]) are located in peri-urban areas or new growing neighborhoods near the outer limits of the city. In addition, the quantile g-computation analysis showed that the socioeconomic characteristics with the higher positive scaled effect size on SUHI estimation were the percentage of people who recently received income and percentage of literacy population per block, with an effect size of 0.687 and 0.313, respectively. The overall mixture effect estimate is -1.01 (confidence interval [CI] 95%: -15.12, 13.09), which is interpreted as the effect on SUHI estimate of increasing every socioeconomic characteristic by one quantile (table 2). When quantile q-computation was stratified by zones, the highest scaled effect size on SUHI estimates per zones were the percentage of literacy population per block in Callao, Center and South

zones (1.000), percentage of people with higher education level per block in North zone (0.808), and percentage of access to health insurance per block (0.528). In Center zone, the percentage of access to health insurance and percentage of people who recently received income per block showed an opposite scaled effect size compared to the other zones. In North zone, percentage of people with higher education level and access to internet service showed an opposite scaled effect size compared to other zones (figure 6).

## 4. Discussion

### 4.1. Main findings

This study quantifies the SUHI at a granular geographic level in Metropolitan Lima and its distribution by the socioeconomic characteristics of their population. We found a clustered spatial distribution of both, SUHI and SES in Lima. In addition, our study reveals that populations with a low social, education, economic, and Non-White ethnicity characteristics are exposed to higher levels of SUHI estimations compared to those populations with high socioeconomic characteristics. Even in the same sub-city area, quantile g-computational model evidence different scaled effect size when stratified by Metropolitan Lima zones. Urban adaptation strategies aiming at reducing the burden associated with extreme heat should take into consideration the socioeconomic disadvantaged populations and its disproportionate exposure to SUHI to better design specific adaptation strategies and prevent heat-related health effects, considering within-city variability. Innovative evidence provided by our study highlights SUHI exposure by SES at fine-scale level in the scarce-evidence context of South America; especially in Peru, the most unequal country in the region [71].

### 4.2. SUHI exposure on disadvantaged socioeconomic groups

Previous studies conducted in high-income areas analyzed UHI exposure across different SES characteristics. In China, Wong *et al* [81] found that disadvantaged SES groups were significantly more exposed to UHI, where zones characterized by older population, only high school attainment, low and middle incomes, and certain occupation groups of workers, have odds ratios greater than 1.2. In addition, they highlighted the spatial clusterization of UHI disproportionate exposure by age, income, educational attainment, and occupation at a medium-size administrative level. In 2018 in the USA, Voekel *et al* [82] addressed UHI and SES relationship at a more fine-scale level (census tract) than previous studies, founding that white population are more likely to be exposed to lower UHI amounts (for each 10% increase in the white population, temperature dropped by 0.15 °C). On the other hand,

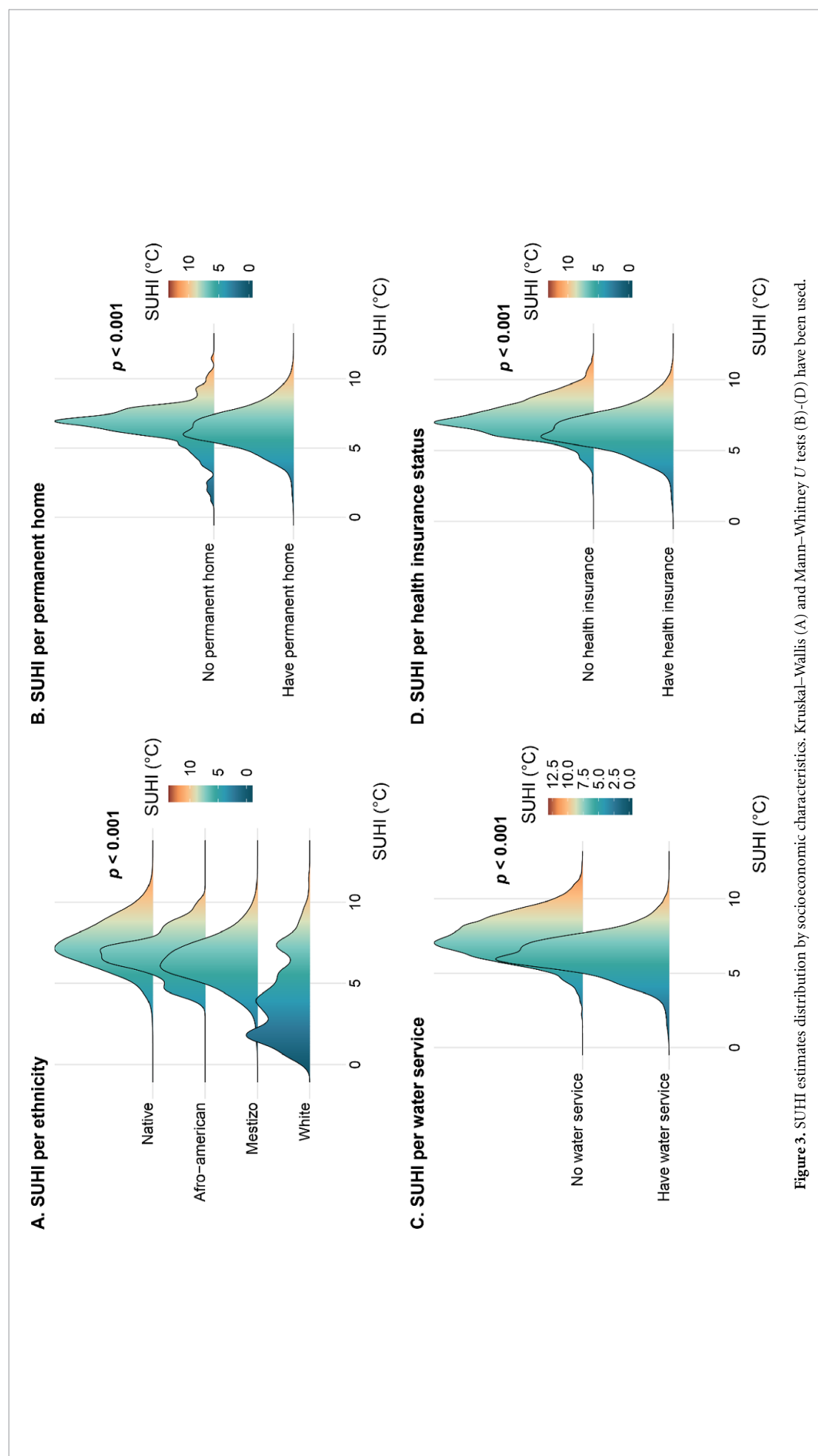
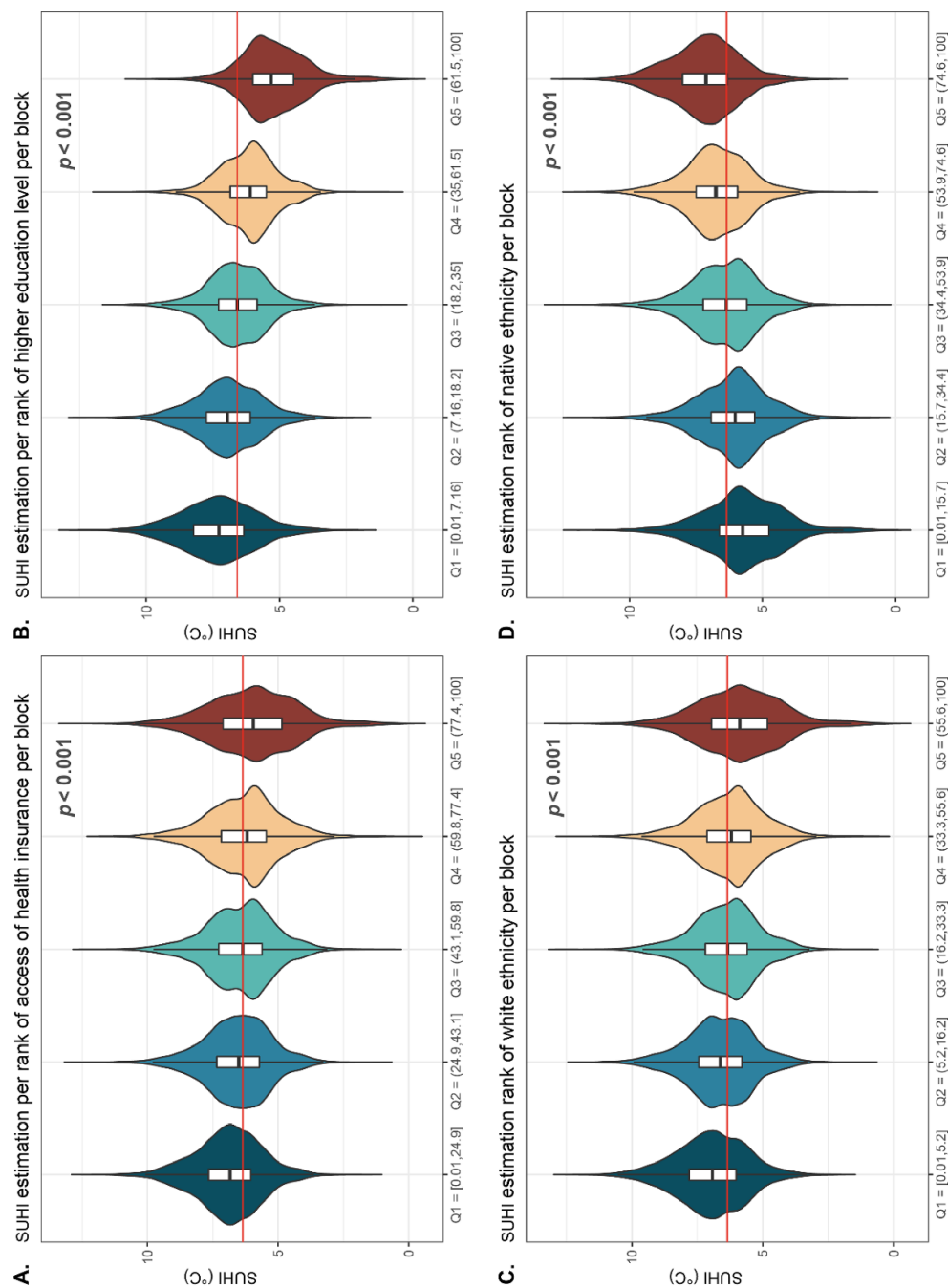
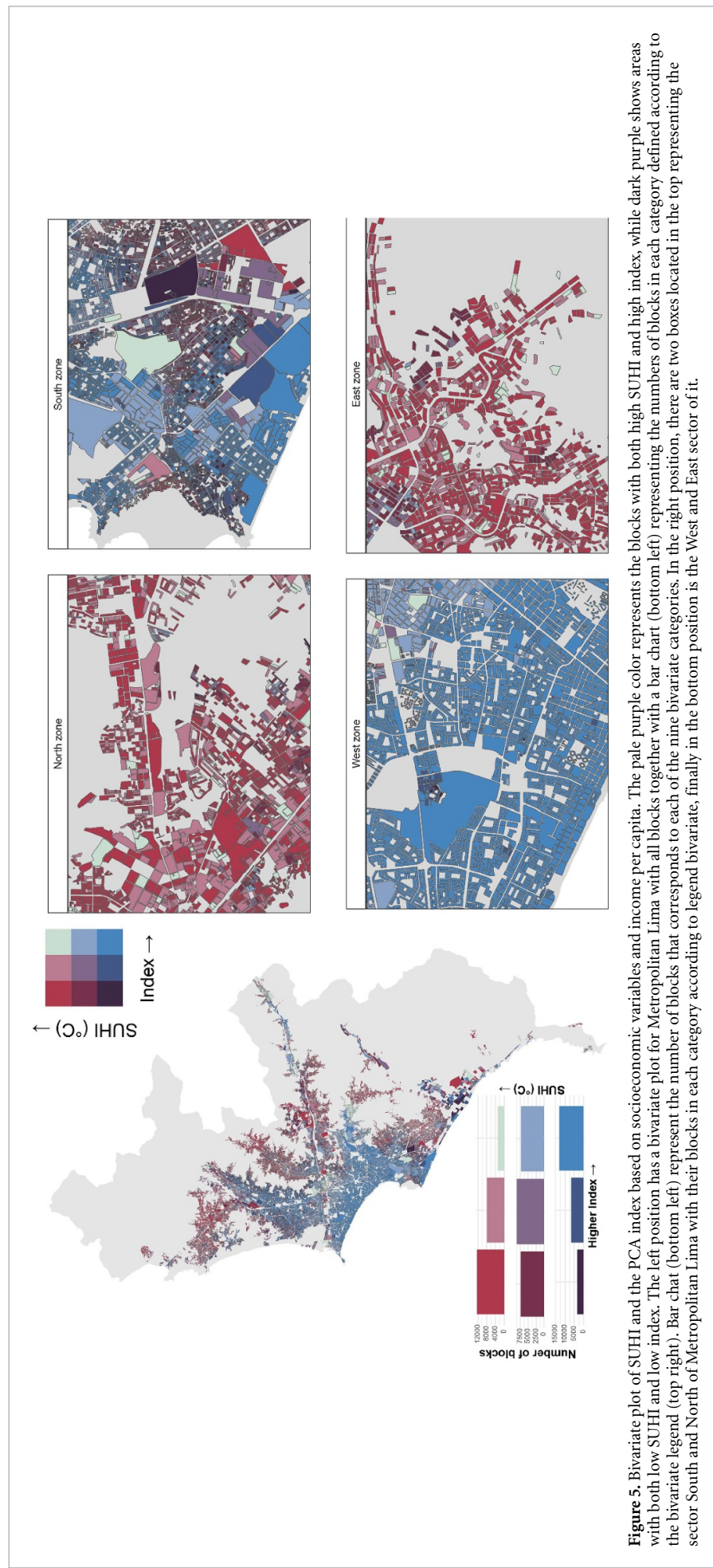


Figure 3. SUHI estimates distribution by socioeconomic characteristics. Kruskal–Wallis (*A*) and Mann–Whitney *U* tests (*B*)–(*D*) have been used.



**Figure 4.** SUHI distribution per rank of socioeconomic characteristics. Kruskal-Wallis has been used to compare groups. Q1-Q5; Quantile 1-5.



**Figure 5.** Bivariate plot of SUHI and the PCA index based on socioeconomic variables and income per capita. The pale purple color represents the blocks with both high SUHI and high index, while dark purple shows areas with both low SUHI and low index. The left position has a bivariate plot for Metropolitan Lima with all blocks together with a bar chart (bottom left) representing the numbers of blocks in each category defined according to the bivariate legend (top right). Bar chart (bottom right) represent the number of blocks that corresponds to each of the nine bivariate categories. In the right position, there are two boxes located in the top representing the sector South and North of Metropolitan Lima with their blocks in each category according to legend bivariate, finally in the bottom position is the West and East sector of it.

Table 2. Quantile g-computation results to estimate the effect of socioeconomic variables on SUHI estimation.

Scaled effect size per socioeconomic variable on SUHI							
% of people who recently received income per block	% of literacy population per block	% of permanent address at house or apartment per block	% of access to electric energy service per block	% of people who are at least 15 years old and able to work per block	% of access to health insurance per block	% of access to internet service per block	
0.687	0.313	0.000	-0.026	-0.058	-0.107	-0.107	
Mixture slope parameters							
Overall mixture effect	Estimate	Confidence interval 95%					
	-1.015 863	-15.1234–13.092					

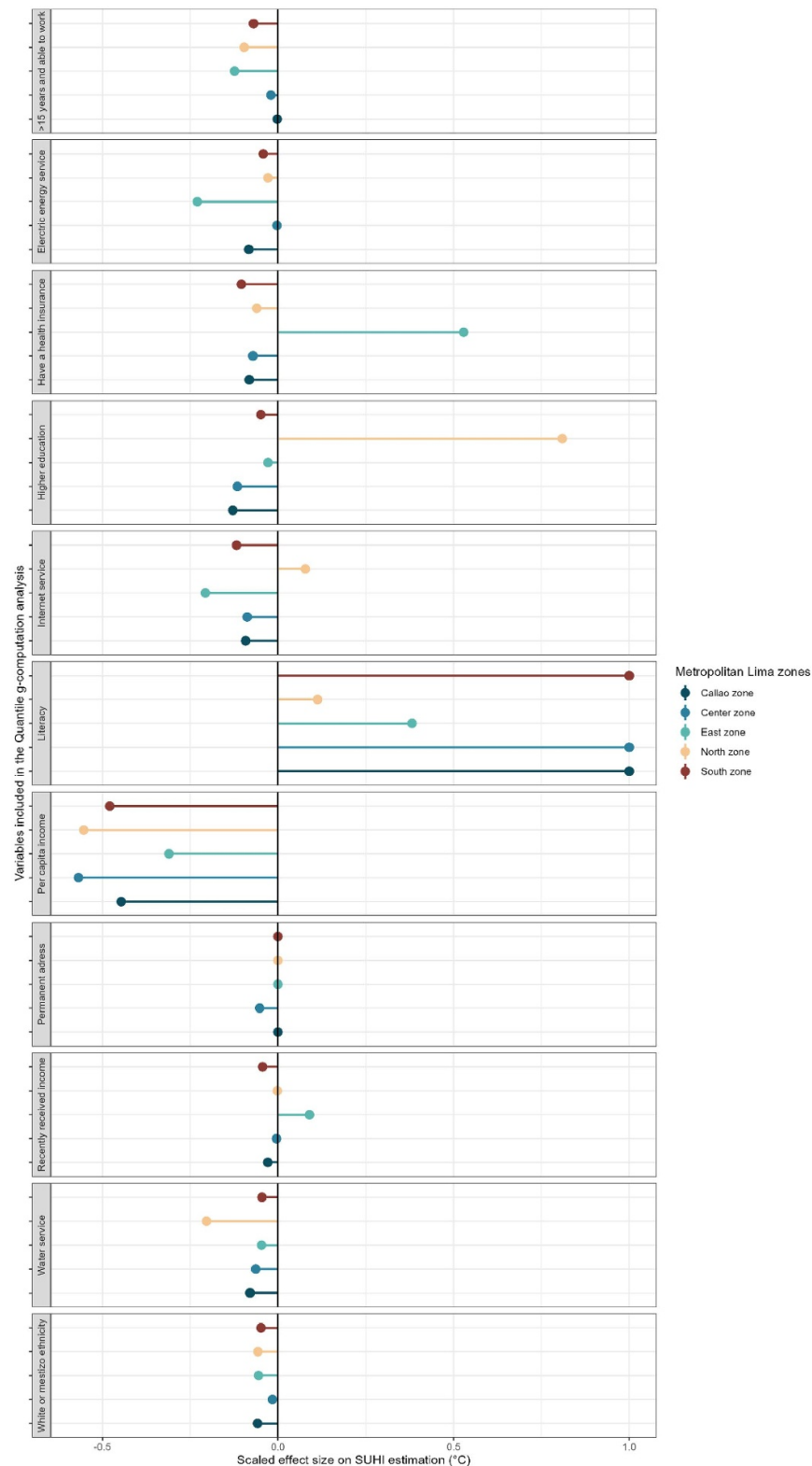


**Figure 6.** Scaled effect size of each socioeconomic variable on SUHI estimation by Metropolitan Lima zones.

they found that Afro-American, Native Hawaiian, Hispanics, and young children populations show a positive linear association with UHI. These studies support our findings, highlighting the importance of SES disproportionate exposure to heat in urban Latin American country settings. Additionally, in our study,

we focused our efforts on downscale spatial resolution (block level) to better understand SES distribution along urban populations.

In terms of health impact, previous studies found that socioeconomic disadvantaged and Non-White ethnicity populations had and excess on heat-related

morbidity and mortality. Yang *et al* [83] estimated that heat-related excess mortality in the illiterate population by 2090 will be 4.4 times greater than 2010 deaths. In the USA, Sharpe and Wolkin [84] found that the extreme weather mortality rate per 100 000 population among American-Indian (or Alaska native) populations compared to white populations was 7.34 times higher. Our results revealed that these populations are exposed to higher levels of SUHI compared to higher SES populations. Therefore, it is logical to point out that high SUHI exposed populations (who are also disadvantaged populations) suffer from increased excess of heat-related mortality. However, more studies are needed to establish a solid relationship between long term SUHI exposure and mortality.

#### 4.3. Urban design impact and SUHI mitigation

The planning and design of public spaces aimed at climate change mitigation and adaptation could result on multiple benefits for human health while reducing social inequalities [85]. Heat-related health impact in urban and non-urban settings can be mitigated by reducing heat accumulation, encourage better building and city design [86]. For example, at the individual level, light clothing, water intake, cool showers, and the use of air conditioner could help [87]. However, not all strategies and approaches are often available to all the population. Vulnerable and poor populations usually do not have permanent access to water and electric energy services [88], making some strategies unfeasible in certain settings. Our findings showed fine-scale heat vulnerable populations who could be considered to long-term adapt heat mitigation strategies.

For example, Raven *et al* [89] and Tong *et al* [86] had suggested how to minimize heat-related effects when building cities. In terms of the urban systems efficiency, the urban waste heat and greenhouse gas emissions from infrastructure and industry can be reduced by changing the form and layout of buildings and its distribution to provide cooling and ventilation, reducing energy use and allowing citizens to cope with higher temperatures and more intense run-off. In addition, when we focus on heat-resistant construction materials, selecting low heat capacity construction materials and reflective coatings can improve building performance by managing heat exchange at the surface. On the other hand, increasing the vegetative cover in a city can simultaneously lower outdoor temperatures, demand for building cooling, and air pollution [86, 89], but the distribution of this vegetation cover, like many other strategies, does not have a homogeneous distribution throughout the city. For example, Astell-Burt *et al* [90] found that areas with a higher percentage of low-income residents are related to less green space availability. It is essential to implement heat mitigation strategies both at individual and urban levels;

however, the same efforts should be made to implement these strategies homogeneously across the city with a special focus on heat-vulnerable populations.

#### 4.4. Strengthen and limitations

It is important to acknowledge the limitations of this study. Our analysis was conducted using cross-sectional data to better characterize the exposure to LST and SUHI, future prospective studies are recommended to understand the unequal disproportionate exposure to SUHI. In addition, only static measures of heat exposure (at home) were considered in this study. However, its dynamic exposure due to human mobility (i.e. commuting to work during the day and returning home at night, or travel to different regions by weeks or months) might show a different pattern in relation to the socio-economic characteristics explored in this study. In addition, it is important to note here that the UHI values observed by satellites and those based on air temperature measurements can be very different [91–93]. It would depend on the composition and humidity of the air, and the type of surfaces in the study zones. Finally, SUHI estimation was based on LST, a not greening based metric which could limit the real heat impact on population. In this paper, we focused on the characterization of MHI using LST variations. However, different land cover land use characteristics (such as level of greenness or the type of materials used in urban surfaces) may differentially drive the distribution of MHI in urban contexts. In future work, it would be interesting to explore the specific drivers of the spatial distribution of MHI in Lima and other geographical contexts.

### 5. Conclusion

We found a SUHI mean estimation per block of 6.44 °C and a clustered spatial distribution of both, SUHI and SES in Lima. In addition, our study highlighted that populations with low SES are more likely to be exposed to higher levels of LST and SUHI estimations compared to those who have a higher SES. We illustrate that this is a very micro-geographic phenomenon and within-city variations should be taken into consideration. Our results could improve environmental health policies to early detect heat-vulnerable populations and tailor specific interventions to prevent heat-related effects and mortality.

### Data availability statement

The data that support the findings of this study are openly available at the following URL/DOI: <https://github.com/healthinnovation/MHI>.

### ORCID iDs

Edson J Ascencio  <https://orcid.org/0000-0002-8340-9236>

- Antony Barja  <https://orcid.org/0000-0001-5921-2858>
- Tarik Benmarhnia  <https://orcid.org/0000-0002-4018-3089>
- Gabriel Carrasco-Escobar  <https://orcid.org/0000-0002-6945-0419>

## References

- [1] Change IC 2013 *The Physical Science Basis* (Washington, DC: Cambridge University Press)
- [2] Pörtner H O, Roberts D C, Adams H, Adler C, Aldunce P, Ali E, Begum R A, Betts R, Kerr R B and Biesbroek R 2022 *Climate Change 2022: Impacts, Adaptation and Vulnerability* (Cambridge: Cambridge University Press)
- [3] Stanev E V and Peneva E L 2001 Regional sea level response to global climatic change: Black Sea examples *Glob. Planet. Change* **32** 33–47
- [4] World Health O 2014 *Quantitative Risk Assessment of the Effects of Climate Change on Selected Causes of Death, 2030s and 2050s* (Geneva: World Health Organization)
- [5] Parry L, Radel C, Adamo S B, Clark N, Counterman M, Flores-Yeffal N, Pons D, Romero-Lankao P and Vargo J 2019 The (in)visible health risks of climate change *Soc. Sci. Med.* **241** 112448
- [6] Manderson L, Aagaard-Hansen J, Allotey P, Gyapong M and Sommerfeld J 2009 Social research on neglected diseases of poverty: continuing and emerging themes *PLoS Negl. Trop. Dis.* **3** e332
- [7] Ebi K L et al 2021 Hot weather and heat extremes: health risks *The Lancet* **398** 698–708
- [8] Burkart K G et al 2021 Estimating the cause-specific relative risks of non-optimal temperature on daily mortality: a two-part modelling approach applied to the global burden of disease study *The Lancet* **398** 685–97
- [9] Ravallion M 2014 Income inequality in the developing world *Science* **344** 851–5
- [10] World Development Indicators 2017 *The World Bank Open Knowledge Repository* (available at: <https://openknowledge.worldbank.org/handle/10986/26447>)
- [11] Feron S et al 2019 Observations and projections of heat waves in South America *Sci. Rep.* **9** 8173
- [12] Gonzales G F, Zevallos A, Gonzales-Castaneda C, Nunez D, Gastanaga C, Cabezas C, Naehler L, Levy K and Steenland K 2014 Environmental pollution, climate variability and climate change: a review of health impacts on the Peruvian population *Rev. Peru. Med. Exp. Salud Publica* **31** 547–56
- [13] Vicedo-Cabrera A M et al 2021 The burden of heat-related mortality attributable to recent human-induced climate change *Nat. Clim. Change* **11** 492–500
- [14] Kephart J L et al 2022 City-level impact of extreme temperatures and mortality in Latin America *Nat. Med.* **28** 1700–5
- [15] Liu Z, Zhan W, Bechtel B, Voogt J, Lai J, Chakraborty T, Wang Z-H, Li M, Huang F and Lee X 2022 Surface warming in global cities is substantially more rapid than in rural background areas *Commun. Earth Environ.* **3** 1–9
- [16] Oke T R 1973 City size and the urban heat island *Atmos. Environ.* **7** 769–79
- [17] Oke T R 1982 The energetic basis of the urban heat island Q. *J. R. Meteorol. Soc.* **108** 1–24
- [18] Gallo K P, McNab A L, Karl T R, Brown J F, Hood J J and Tarpley J D 1993 The use of NOAA AVHRR data for assessment of the urban heat island effect *J. Appl. Meteorol.* **32** 899–908
- [19] Sen Roy S and Yuan F 2009 Trends in extreme temperatures in relation to urbanization in the twin cities Metropolitan area, Minnesota *J. Appl. Meteorol. Climatol.* **48** 669–79
- [20] Graff Zivin J and Neidell M 2014 Temperature and the allocation of time: implications for climate change *J. Labor Econ.* **32** 1–26
- [21] Heal G and Park J 2016 Temperature stress and the direct impact of climate change: a review of an emerging literature *Rev. Environ. Econ. Policy* **10** 1–17
- [22] Heaviside C, Macintyre H and Vardoulakis S 2017 The urban heat island: implications for health in a changing environment *Curr. Environ. Health Rep.* **4** 296–305
- [23] Park R J 2022 Hot temperature and high-stakes performance *J. Hum. Resour.* **57** 400–34
- [24] Shahmohamadi P, Che-Ani A I, Etessam I, Maulud K N A and Tawil N M 2011 Healthy environment: the need to mitigate urban heat island effects on human health *Proc. Eng.* **20** 61–70
- [25] Tan J, Zheng Y, Tang X, Guo C, Li L, Song G, Zhen X, Yuan D, Kalkstein A J and Li F 2010 The urban heat island and its impact on heat waves and human health in Shanghai *Int. J. Biometeorol.* **54** 75–84
- [26] Anderson G B and Bell M L 2011 Heat waves in the United States: mortality risk during heat waves and effect modification by heat wave characteristics in 43 U.S. communities *Environ. Health Perspect.* **119** 210–8
- [27] Antonia K, Glen P K and Andreas D F 2018 The impact of heat waves on mortality among the elderly: a mini systematic review *J. Geriatr. Med. Gerontol.* **4** 053
- [28] Burke M, González F, Baylis P, Heft-Neal S, Baysan C, Basu S and Hsiang S 2018 Higher temperatures increase suicide rates in the United States and Mexico *Nat. Clim. Change* **8** 723–9
- [29] Madrigano J, Mittleman M A, Baccarelli A, Goldberg R, Melly S, von Klot S and Schwartz J 2013 Temperature, myocardial infarction, and mortality: effect modification by individual- and area-level characteristics *Epidemiology* **24** 439–46
- [30] Wang Y et al 2019 Tens of thousands additional deaths annually in cities of China between 1.5 degrees C and 2.0 degrees C warming *Nat. Commun.* **10** 3376
- [31] UNSD 2019 *Demographic Yearbook 2019* (New York: United Nations, Statistics Division)
- [32] Programme UNHS 2010 *State of the World's Cities 2010/2011: Bridging the Urban Divide* (London: Earthscan)
- [33] Gronlund C J 2014 Racial and socioeconomic disparities in heat-related health effects and their mechanisms: a review *Curr. Epidemiol. Rep.* **1** 165–73
- [34] Abreu M and Assis W L 1998 A ilha de calor em Belo Horizonte: um estudo de caso
- [35] Aceituno P and Ulriksen P 1981 Efecto de isla calórica en Santiago. Resultados preliminares *Tralca* **2** 39–56
- [36] Ángel L, Ramírez A and Domínguez E 2010 Isla de calor y cambios espacio-temporales de la temperatura en la ciudad de Bogotá *Rev. Acad. Colomb. Cienc.* **34** 173–83
- [37] Barros H R and Lombardo M A 2016 A ilha de calor urbana e o uso e cobertura do solo no município de São Paulo-SP *GEOUSP: Espaço e Tempo* **20** 160–77
- [38] Caicedo J D P, Pulido S I, Rodríguez O J and Mendivilo J C 1998 Análisis preliminar de la isla de calor en la Sabana de Bogotá *Cuadernos de Geografía* **7** 87–93
- [39] Camilloni I and Barrucand M 2011 Temporal variability of the Buenos Aires, Argentina, urban heat island *Theor. Appl. Climatol.* **107** 47–58
- [40] Camilloni IA 1995 Detección de la señal de la isla urbana de calor y de variaciones climáticas (Universidad de Buenos Aires Facultad de Ciencias Exactas y Naturales)
- [41] Cui Y Y and De Foy B 2012 Seasonal variations of the urban heat island at the surface and the near-surface and reductions due to urban vegetation in Mexico City *J. Appl. Meteorol. Climatol.* **51** 855–68
- [42] de Almeida Magalhães Filho L C and de Abreu J F 2010 Ilha de calor urbana, metodologia para mensuração: belo Horizonte, uma análise exploratória *Revista de Biologia e Ciências da Terra* **10** 1–24

- [43] Ferreira M J, de Oliveira A P and Soares J 2013 Diurnal variation in stored energy flux in São Paulo city, Brazil *Urban Clim.* **5** 36–51
- [44] Figueroa P I and Mazzeo N A 1998 Urban-rural temperature differences in Buenos Aires *Int. J. Climatol.* **18** 1709–23
- [45] Forsberg V S S and Párraga E O 2016 Identificación de islas de calor en la ciudad de Lima Metropolitana utilizando imágenes del Satélite Landsat 5TM *An. científicos* **77** 34–44
- [46] Jauregui E 1973 The urban climate of Mexico City *Erdkunde* **27** 298–307
- [47] Jauregui E 1997 Heat island development in Mexico City *Atmos. Environ.* **31** 3821–31
- [48] Jáuregui E 2000 *El clima de la ciudad de México* vol 1 (Mexico: Plaza y Valdés)
- [49] Lombardo M A 1985 Ilha de calor nas metrópoles: o exemplo de São Paulo (Editora Hucitec com apoio de Laleklá SA Comércio e Indústria)
- [50] Lucena A, Rotunno Filho O C, França J, Peres L and Xavier L N R 2012 Urban climate and clues of heat island events in the Metropolitan area of Rio de Janeiro *Theor. Appl. Climatol.* **111** 497–511
- [51] Marques Filho E P, Karam H A, Miranda A G and França J 2009 Rio de Janeiro's tropical urban climate *News Lett. Int. Assoc. Urban Clim.* **32** 5–9
- [52] Molina M 2007 Efectos de los tipos de urbanización asociados al crecimiento urbano del área metropolitana de Santiago sobre la generación y comportamiento de micro islas de calor *Memoria de título Geografía, Universidad de Chile, Departamento de Geografía, Santiago*
- [53] Roth M 2007 Review of urban climate research in (sub)tropical regions *Int. J. Climatol.* **27** 1859–73
- [54] Rusticucci M and Vargas W 1991 Efecto de la ciudad y el río sobre la temperatura de superficie en Buenos Aires *Geoacta* **18** 35–48
- [55] Salinas F 1982 Estudio experimental del efecto de isla calórica en la ciudad de Santiago (Memoria para optar título Ing Civil, Universidad de Chile, Santiago, Chile) p 254
- [56] Sarricolea P, Herrera-Ossandon M and Meseguer-Ruiz Ó 2016 Climatic regionalisation of continental Chile *J. Maps* **13** 66–73
- [57] Sena C A P, JRdA F and Peres L F 2014 Estudo da Ilha de Calor na Região Metropolitana do Rio de Janeiro usando dados do MODIS *Anuário do Instituto de Geociências* **37** 111–22
- [58] Smith P and Romero H 2016 Factores explicativos de la distribución espacial de la temperatura del aire de verano en Santiago de Chile *Revista de geografía Norte Grande* **63** 45–62
- [59] Palme M and Carrasco C 2022 Chapter 12—urban heat island in Latin American cities: a review of trends, impacts, and mitigation strategies *Global Urban Heat Island Mitigation* ed A Khan, H Akbari, F Fiorito, S Mithun and D Niyogi (Amsterdam: Elsevier) pp 251–67
- [60] Palme M, Inostroza L, Villacreses G, Lobato-Cordero A and Carrasco C 2017 From urban climate to energy consumption. Enhancing building performance simulation by including the urban heat island effect *Energy Build.* **145** 107–20
- [61] Palme M, Lobato A and Carrasco C 2016 Quantitative analysis of factors contributing to urban heat island effect in cities of Latin-American pacific coast *Proc. Eng.* **169** 199–206
- [62] Inostroza L and Csaplovics E 2014 Measuring climate change adaptation in Latin-America. Spatial indexes for exposure, sensitivity and adaptive capacity to urban heat islands in Lima and Santiago de Chile *Lincoln Institute working paper*
- [63] Turek-Hankins L L et al 2021 Climate change adaptation to extreme heat: a global systematic review of implemented action *Oxford Open Clim. Change* **1** kgab005
- [64] Stone B Jr, Vargo J, Liu P, Hu Y and Russell A 2013 Climate change adaptation through urban heat management in Atlanta, Georgia *Environ. Sci. Technol.* **47** 7780–6
- [65] White-Newsome J, O'Neill M S, Gronlund C, Sunbury T M, Brines S J, Parker E, Brown D G, Rood R B and Rivera Z 2009 Climate change, heat waves, and environmental justice: advancing knowledge and action *Environ. Justice* **2** 197–205
- [66] Fernández-de-córdova G, Moschella P and Fernández-Maldonado A M 2021 Changes in spatial inequality and residential segregation in Metropolitan Lima *Urban Socio-Economic Segregation and Income Inequality: A Global Perspective* ed M van Ham, T Tammaru, R Ubarevičienė and H Janssen (Cham: Springer) pp 471–90
- [67] Degefu M A, Argaw M, Feyisa G L and Degefa S 2022 Regional and urban heat island studies in megacities: a systematic analysis of research methodology *Indoor Built Environ.* **31** 1775–86
- [68] Dong P, Jiang S, Zhan W, Wang C, Miao S, Du H, Li J, Wang S and Jiang L 2022 Diurnally continuous dynamics of surface urban heat island intensities of local climate zones with spatiotemporally enhanced satellite-derived land surface temperatures *Build. Environ.* **218** 109105
- [69] Liao Y, Shen X, Zhou J, Ma J, Zhang X, Tang W, Chen Y, Ding L and Wang Z 2022 Surface urban heat island detected by all-weather satellite land surface temperature *Sci. Total Environ.* **811** 151405
- [70] Tariq A, Mumtaz F, Zeng X, Baloch M Y J and Moazzam M F U 2022 Spatio-temporal variation of seasonal heat islands mapping of Pakistan during 2000–2019, using day-time and night-time land surface temperatures MODIS and meteorological stations data *Remote Sens. Appl.* **27** 100779
- [71] Chancel L, Piketty T, Saez E and Zucman G 2022 World Inequality Report 2022
- [72] INEI 2007 Instituto nacional de estadística e informática-INEI-Perú
- [73] Beck H E, van Dijk A I J M, de Roo A, Miralles D G, McVicar T R, Schellekens J and Bruijnzeel L A 2016 Global-scale regionalization of hydrologic model parameters *Water Resour. Res.* **52** 3599–622
- [74] Icochea Iriarte F SENAMHI—Perú (available at: [www.senamhi.gob.pe/?&p=estaciones](http://www.senamhi.gob.pe/?&p=estaciones))
- [75] Zerpa Tawara N and Gutierrez Zapata M Ministerio de Salud—Direcciones de Redes Integradas de Salud (DIRIS) (available at: [www.gob.pe/21128-ministerio-de-salud-direcciones-de-redes-integradas-de-salud-diris](http://www.gob.pe/21128-ministerio-de-salud-direcciones-de-redes-integradas-de-salud-diris))
- [76] Gorelick N, Hancher M, Dixon M, Ilyushchenko S, Thau D and Moore R 2017 Google earth engine: planetary-scale geospatial analysis for everyone *Remote Sens. Environ.* **202** 18–27
- [77] Ermida S L, Soares P, Mantas V, Götsche F-M and Trigo I F 2020 Google earth engine open-source code for land surface temperature estimation from the landsat series *Remote Sens.* **12** 1471
- [78] McCartney S M, Shandas A, Gallo V, Paris K, Nix G, Quintero S, Tomlinson T and Xian A G 2020 (available at: <https://appliedsciences.nasa.gov/join-mission/training/english/asset-satellite-remote-sensing-urban-heat-islands>)
- [79] Bernasocchi M, Pasotti A and Neumann A Zonal statistics (available at: [https://docs.qgis.org/2.8/en/docs/user\\_manual/processing\\_algs/qgis/raster\\_tools/zonalstatistics.html](https://docs.qgis.org/2.8/en/docs/user_manual/processing_algs/qgis/raster_tools/zonalstatistics.html))
- [80] Keil A P, Buckley J P, O'Brien K M, Ferguson K K, Zhao S and White A J 2020 A quantile-based g-computation approach to addressing the effects of exposure mixtures *Environ. Health Perspect.* **128** 47004
- [81] Wong M S, Peng F, Zou B, Shi W Z and Wilson G J 2016 Spatially analyzing the inequity of the Hong Kong urban heat island by socio-demographic characteristics *Int. J. Environ. Res. Public Health* **13** 317
- [82] Voelkel J, Hellman D, Sakuma R and Shandas V 2018 Assessing vulnerability to urban heat: a study of disproportionate heat exposure and access to refuge by socio-demographic status in Portland, Oregon *Int. J. Environ. Res. Public Health* **15** 640
- [83] Yang J et al 2021 Projecting heat-related excess mortality under climate change scenarios in China *Nat. Commun.* **12** 1039

- [84] Sharpe J D and Wolkin A F 2022 The epidemiology and geographic patterns of natural disaster and extreme weather mortality by race and ethnicity, United States, 1999–2018 *Public Health Rep.* **137** 1118–25
- [85] Ganzleben C and Kazmierczak A 2020 Leaving no one behind—understanding environmental inequality in Europe *Environ. Health* **19** 57
- [86] Tong S, Prior J, McGregor G, Shi X and Kinney P 2021 Urban heat: an increasing threat to global health *BMJ* **375** n2467
- [87] World Health O 2011 *Public Health Advice on Preventing Health Effects of Heat: New and Updated Information for Different Audiences* (Copenhagen: World Health Organization, Regional Office for Europe)
- [88] Mechanic D and Tanner J 2007 Vulnerable people, groups, and populations: societal view *Health Aff.* **26** 1220–30
- [89] Raven J, Stone B, Mills G, Towers J, Katzschnier L, Leone M F, Gaborit P, Georgescu M, Hariri M and Lee J 2018 Urban planning and urban design *Climate Change and Cities:* Second Assessment Report of the Urban Climate Change Research Network ed C Rosenzweig, P Romero-Lankao, S Mehrotra, S Dhakal, S Ali Ibrahim and W D Solecki (Cambridge: Cambridge University Press) pp 139–72
- [90] Astell-Burt T, Feng X, Mavoa S, Badland H M and Giles-Corti B 2014 Do low-income neighbourhoods have the least green space? A cross-sectional study of Australia's most populous cities *BMC Public Health* **14** 292
- [91] Chakraborty T, Sarangi C and Tripathi S N 2016 Understanding diurnality and inter-seasonality of a sub-tropical urban heat island *Bound.-Layer Meteorol.* **163** 287–309
- [92] Hu Y, Hou M, Jia G, Zhao C, Zhen X and Xu Y 2019 Comparison of surface and canopy urban heat islands within megacities of eastern China *ISPRS J. Photogramm. Remote Sens.* **156** 160–8
- [93] Venter Z S, Chakraborty T and Lee X 2021 Crowdsourced air temperatures contrast satellite measures of the urban heat island and its mechanisms *Sci. Adv.* **7** eabb9569